Delays in Activity-Based Neural Networks

Oliver Thomas-Roche

University of Nottingham
UK | CHINA | MALAYSIA

1. Introduction

Delays are ubiquitous in neural networks, arising during action potential propagation, pre- and post-synaptic signal transduction, and dendritic signal propagation. Such delays are commonly associated with generating oscillations and bursting in spiking neural networks.

Coombes and Laing [1] apply two discrete delays to a Wilson-Cowan network [2] relating to self- and cross-interaction between two populations of neurones. They show that the presence of delays can induce oscillatory behaviour through the destabilisation of fixed points. Moreover, for certain parameter windows, chaotic and quasi-periodic behaviour can emerge.

Analysis for this paper was conducted in MATLAB with the aid of DDE-BIFTOOL [3].

2. The Model

The Wilson-Cowan network [2] takes advantage of the fact that spiking neural networks can be reduced to a minimal number of variables. With the addition of delays, the model takes the form

$$\dot{u} = -u + f(\theta_u + au(t-\tau_1) + bv(t-\tau_2))$$
$$\frac{1}{\alpha}\dot{v} = -v + f(\theta_v + cu(t-\tau_2) + dv(t-\tau_1))$$

where u and v represent the neural activity of two populations. The network weights a and d fix self-interaction strength, while b and c fix cross-interaction strength. $\theta_{u,v}$ describes an external drive to each population while α sets a timescale for response. The firing rate function, $f(z)$, is chosen as a sigmoid with variable steepness set by β. Finally, τ_1 and τ_2 differentiate self-interaction delays with cross-interaction delays.

By analysing the trace and determinant of the Jacobian of the system without delays, Hopf, saddle-node, and Bogdanov-Takens bifurcations can be calculated - shown in *figure 1*. Sections of saddle-node bifurcations between both Hopf branches are classified as saddle-node on an invariant circle (SNIC) bifurcations. Beyond these bifurcations, oscillations are destroyed. Therefore, within this central region (OR) – between Hopf and SNIC bifurcations – oscillations can occur.

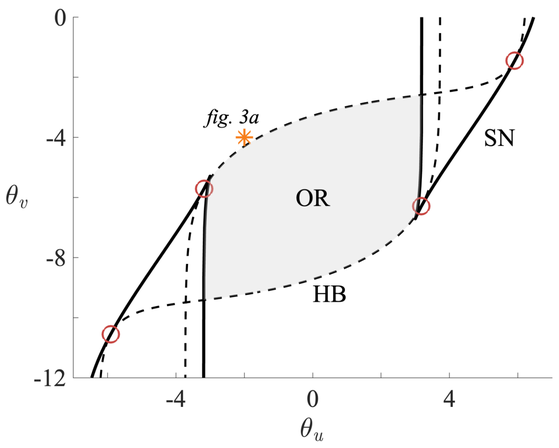

Figure 1. Bifurcation diagram of a Wilson-Cowan network with no delays showing Hopf bifurcations (HB, dashed line), saddle-node bifurcations (SN, solid line), and Bogdanov-Takens bifurcations (red circles). Oscillatory region (OR) is shaded in grey. Parameters are $\alpha = 1, \beta = 1, a = -b = c = 10, d = 2$. Orange star indicates a point in the (θ_u, θ_v) plane used in later simulations (*figure 3a*).

3. Delays & Fixed Point Stability

Delays in a Wilson-Cowan network [2] do not affect the existence of fixed points but can alter their stability. Real instability of a fixed point in the delayed network is independent of delays and so is identical to the conditions for a saddle-node bifurcation. Dynamic instability, however, requires a pair of complex-conjugate eigenvalues of the Jacobian to cross the imaginary axis – $Re\ \mathcal{E}(\lambda) = 0$. This is evaluated at $\lambda = i\omega$ for $\omega \neq 0$, where $\omega \in \mathbb{R}$ and describes the frequency of oscillations that emerge at the bifurcation.

As seen in *figure 2*, if either delay is sufficiently large, dynamic instability will arise. However, an interference effect can occur where a small region in (τ_1, τ_2) is stable to Hopf bifurcations. If values for $\theta_{u,v}$ are selected within the oscillatory region in *figure 1*, the stable region will become extremely narrow but will not be destroyed.

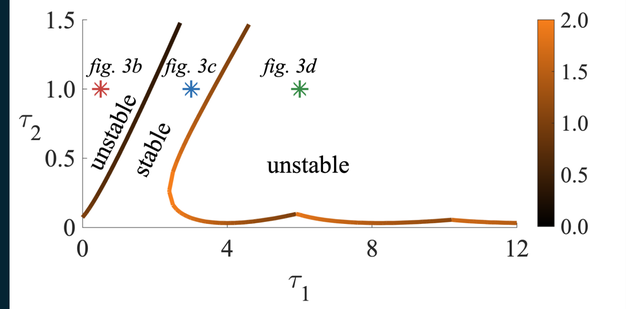

Figure 2. Bifurcation diagram of a delayed Wilson-Cowan network showing fixed point stability in the (τ_1, τ_2) plane. Parameters are $\alpha = 1, \beta = 1, a = -b = c = 10, d = 2, \theta_u = -2, \theta_v = -4$. Colour-bar indicates the range of ω values found at bifurcation points. Coloured stars indicate points used in later simulations *(figure 3)*.

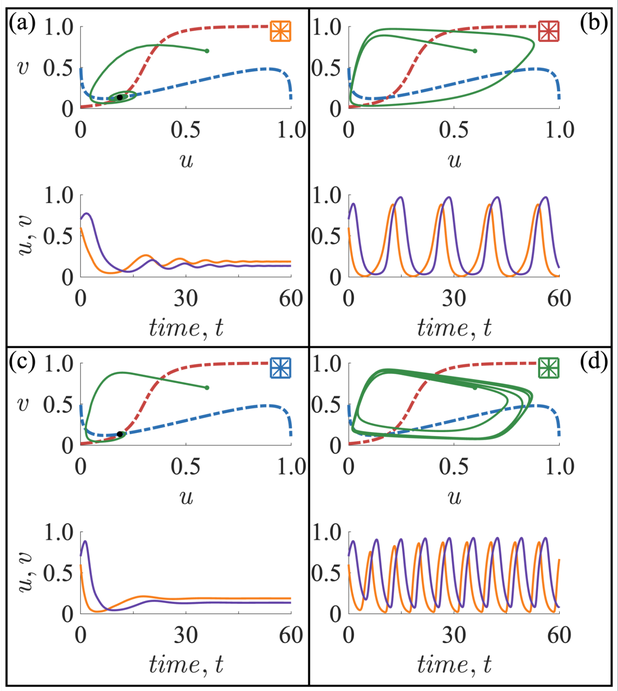

Figure 3. Simulations of the Wilson-Cowan system in the (u, v) plane and (u, v) against time, t, with parameters identical to *figure 2*, at **(a)** $(\tau_1, \tau_2) = (0, 0)$, *figure 1*: orange star, **(b)** $(\tau_1, \tau_2) = (0.5, 1)$, *figure 2*: red star, **(c)** $(\tau_1, \tau_2) = (3, 1)$, *figure 2*: blue star, **(d)** $(\tau_1, \tau_2) = (6, 1)$, *figure 2*: green star. u-nullclines (red dashed line) and v-nullclines (blue dashed line) shown alongside solutions in (u, v) (green line) as well as u against time (orange line) and v against time (purple line). Black dots denote stable fixed points.

4. Bifurcation Analysis

By varying $\theta_{u,v}$ and $\tau_1 = \tau_2 = \tau$, using DDE-BIFTOOL [3], saddle-node and Hopf bifurcations of fixed points can be detected and followed in this parameter space. It is also possible to construct oscillations around Hopf bifurcations to follow stable and unstable branches of these oscillations and detect corresponding saddle-node bifurcations. Fixing $\theta_v = 0.5$, provides a typical bifurcation diagram in (θ_u, τ) space shown in *figure 4*. Further, *figure 5*, depicts cross-sections of *figure 4*. When $\tau > 0.35$, a branch of stable oscillations links Hopf bifurcations. Between $\tau = 0.35$ and $\tau = 0.1$ a pair of saddle-node bifurcations of these oscillations arises, creating a branch of unstable oscillations. When $\tau < 0.1$, Hopf bifurcations pass the saddle-point to occur on the middle branch, giving rise to a single unstable branch of oscillations.

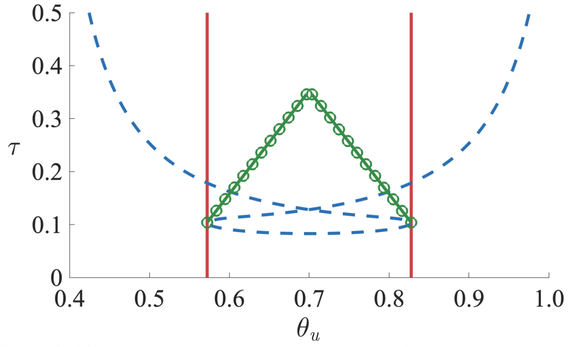

Figure 4. Bifurcation diagram showing saddle-node bifurcations (red line), Hopf bifurcations (blue dashed line), and saddle-node bifurcations of oscillations (circles joined by green line). Parameters are $\alpha = 1, \beta = 60, a = c = -1$, b $= -0.4, d = 0, \theta_v = 0.5$.

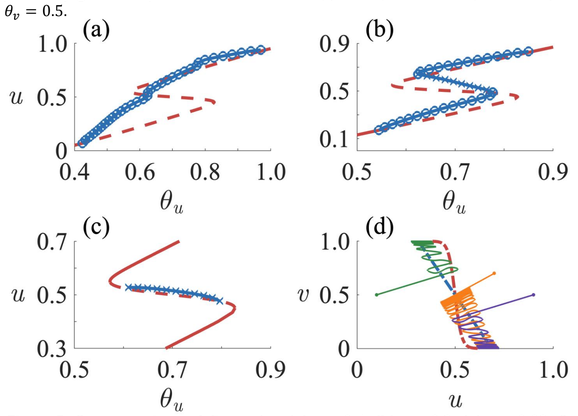

Figure 5. Cross-sections of *figure 4* at **(a)** $\tau = 0.5$, **(b)** $\tau = 0.2$, **(c)** $\tau = 0.09$. Stable fixed points (red line), unstable fixed points (red dashed line), stable oscillations (circles joined by blue line), and unstable oscillations (crosses joined by blue line) are shown. Maximum u over a single oscillation is plotted. Parameters are identical to *figure 4*. **(d)** Simulations in the (u, v) plane. Parameters are identical to *figure 4*, with $\theta_u = 0.7, \tau = 0.2$. u-nullcline (red dashed line) and v-nullcline (blue dashed line) shown alongside solutions with starting points (0.1,0.5) – green line, (0.7,0.7) – orange line, and (0.9,0.5) – purple line. Orange line shows bursting activity around central unstable fixed point, followed by oscillations moving towards and stabilising around the lower fixed point.

5. Chaos and Quasi-Periodicity

Coombes and Laing [2] show that using numerical simulation we can probe the delayed Wilson-Cowan model for chaotic and quasi-periodic behaviour. For a typical chaotic solution, shown in *figure 6a*, decreasing the steepness of the firing rate function, β, induces a shift to quasi-periodicity, shown in *figure 6b*.

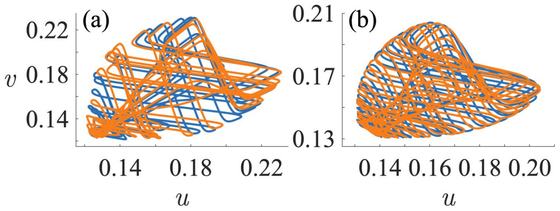

Figure 6. **(a)** a chaotic solution and **(b)** a quasi-periodic solution with starting points $(0.1313, 0.15)$ – blue line, and $(0.1323, 0.15)$ – orange line. Parameters are $\alpha = 1, a = d = -3.7$, b $= c = 1.9, \theta_u = \theta_v = 0.2, \tau_1 = \tau_2 = 0.1$, **(a)** $\beta = 60$, **(b)** $\beta = 40$.

To evaluate chaos in this system, we can approximate the maximum Lyapunov exponent for a given set of parameters. Given a solution with a set history, I introduce a perturbation at each time point and integrate this perturbed solution to the next time point. Logarithm rate of growth is calculated from the distance between the two solutions at this next time point. This is repeated and averaged over the whole solution to approximate the maximum Lyapunov exponent. The results of this are shown in *figure 7* and highlight a single fixed point that undergoes a Hopf bifurcation along the outer edge of Lyapunov exponents.

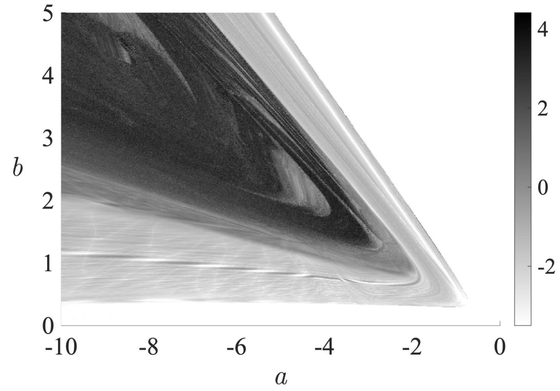

Figure 7. Approximated maximum Lyapunov exponents. Outer edge of shaded region signifies a Hopf bifurcation, beyond which (in white) there is a stable fixed point. Higher Lyapunov exponents signify chaotic behaviour. Parameters are $\alpha = 1, \beta = 60$, $a = d$, b $= c, \theta_u = \theta_v = 0.2, \tau_1 = \tau_2 = 0.1$.

6. Discussion

Incorporating delays into neural models greatly enhances their match with spiking networks [4] due to their abundance in natural systems [1]. In *figure 2* and *3*, we show how delays can generate oscillations in previously stable systems and in *figure 4* and *5* we dissect how such oscillations are generated and destroyed. Between saddle-node bifurcations in *figure 4* we observe three steady states that can support bursting due to an unstable branch of oscillations surrounded by stable oscillations (*figure 5b, d*).

Exploring neurological rhythms *in silico* will allow a greater understanding of the impact of arrythmias in the brain present in diseases such as epilepsy [5]. However, future work should incorporate distributed delays along with less simplified synaptic properties and connectivity patterns to approximate natural systems more reliably and provide a better understanding of the dynamics at play in real brain activity.

7. References

[1] Coombes, S. & Laing, C. (2009). Delays in activity-based neural networks. Philosophical Transactions of the Royal Society A: Mathematical, Physical and Engineering Sciences, 367, 1117-1129.

[2] Wilson, H. R. & Cowan, J. D. (1973). A mathematical theory of the functional dynamics of cortical and thalamic nervous tissue. Kybernetik, 13, 55-80.

[3] Engelborghs, K., Luzyanina, T. & Roose, D. (2002). Numerical bifurcation analysis of delay differential equations using DDE-BIFTOOL. ACM Trans. Math. Softw., 28, 1–21.

[4] Roxin, A., Brunel, N. & Hansel, D. (2005). Role of Delays in Shaping Spatiotemporal Dynamics of Neuronal Activity in Large Networks. Physical Review Letters, 94, 238103.

[5] Wu, Y., Liu, D. & Song, Z. (2015). Neuronal networks and energy bursts in epilepsy. Neuroscience, 287, 175-186.